MATERIALS SCIENCE

Direct observation of shift and ballistic photovoltaic currents

Aaron M. Burger[1], Radhe Agarwal[2], Alexey Aprelev[3], Edward Schruba[1], Alejandro Gutierrez-Perez[2], Vladimir M. Fridkin[2,4], Jonathan E. Spanier[1,2,3]*

The quantum phenomenon of shift photovoltaic current was predicted decades ago, but this effect was never observed directly because shift and ballistic currents coexist. The atomic-scale relaxation time of shift, along with the absence of a photo-Hall behavior, has made decisive measurement of shift elusive. Here, we report a facile, direct-current, steady-state method for unambiguous determination of shift by means of the simultaneous measurements of linear and circular bulk photovoltaic currents under magnetic field, in a sillenite piezoelectric crystal. Comparison with theoretical predictions permits estimation of the signature length scale for shift. Remarkably, shift and ballistic photovoltaic currents under monochromatic illumination simultaneously flow in opposite directions. Disentangling the shift and ballistic contributions opens the way for quantitative, fundamental insight into and practical understanding of these radically different photovoltaic current mechanisms and their relationship.

INTRODUCTION

The bulk photovoltaic current in crystals among 20 symmetry point groups that lack a center of inversion consists of two parts: ballistic and shift photovoltaic currents. Shift photovoltaic current (*1*), which contributes to the bulk photovoltaic effect (BPE) (*2*–*4*), has recently generated substantial interest in solid state science, physical chemistry, optoelectronics, and engineering, in part because this remarkable phenomenon involving inversion symmetry breaking has been proposed as a mechanism for photogenerated current, and because of its possible connections with electronic structure in topological insulators (*5*) and Weyl semimetals (*6*), photovoltaics in the absence of a junction (*7*–*9*), and nonlinear light-matter interactions such as second-harmonic generation (*10*). The BPE is a widely explored phenomenon in noncentrosymmetric materials; violation of the principle of detailed balance in the BPE and its application in nanoscale electrode geometry have yielded unity or higher quantum efficiency, and overcoming of the Shockley-Queisser limit on power conversion efficiency (*11*), not attainable using traditional *p*-*n* junction photovoltaics. Although the quantum phenomenon of shift photovoltaic current was theoretically predicted decades ago (*1*), the atomic-scale relaxation time of shift current (≈0.1 to 1 fs) has made it experimentally inaccessible.

Decades following the experimental discovery of the BPE (*2*, *3*) and subsequent development of theoretical models of ballistic and shift currents (*4*, *12*, *13*), expression of the shift mechanism of the bulk photovoltaic current in the form of a first principles density functional theoretical framework (*14*, *15*) advancing the seminal theoretical description (*1*) has reinvigorated this research, opening the way for materials design and prediction of shift current excitations (*16*, *17*). In a number of recent experimental works (*18*–*24*), it has been reported that the shift mechanism may be responsible for any photovoltaic current in a crystal lacking inversion symmetry and may account for enhanced BPE (*25*, *26*) and even anomalously large carrier collection length arising from local excitation (*23*, *24*, *27*).

[1]Department of Electrical and Computer Engineering, Drexel University, Philadelphia, PA 19104, USA. [2]Department of Materials Science and Engineering, Drexel University, Philadelphia, PA 19104, USA. [3]Department of Physics, Drexel University, Philadelphia, PA 19104, USA. [4]Shubnikov Institute of Crystallography, Russian Academy of Sciences, Leninsky Prospect 59, Moscow, 117333, Russian Federation. *Corresponding author. Email: spanier@drexel.edu

Uniform illumination of a homogeneous asymmetric optically active crystal permits observation of the bulk photovoltaic current $j_i = G^l_{ijk} e_j e^*_k I + iG^c_{ik}[ee^*]_k I$, where the first part is the linear bulk photovoltaic current, obtained with linearly polarized light, the second part is the circular photovoltaic current, obtained using circularly polarized light, I is the light intensity, e_j and e^*_k are the components of the incident light polarization vector, $i[ee^*]$ determines the degree of circular polarization σ, and G^l_{ijk} and G^c_{ik} are third and second rank tensors; $i[ee^*] = \sigma\vec{q}/|q|$, where q is the photon wave vector. This phenomenon was termed the BPE, and the first experimental observations of the linear BPE were in ferroelectrics SbSI (point group C_{2v}) (*2*) and $LiNbO_3$ (C_{3v}) (*3*), and of the circular BPE, in Te (D_3) (*28*, *29*). A comprehensive review of the theories of the linear and circular BPEs in a broad group of ferroelectrics and piezoelectrics has been presented (*4*).

The microscopic nature of the BPE is related to two mechanisms: ballistic and shift. The ballistic mechanism is associated with the excitation of nonthermalized (hot) carriers in a noncentrosymmetric crystal, leading to an asymmetric distribution of hot carrier momenta in the band and a violation of the Boltzmann principle of detailed balance (*4*). In the ballistic mechanism, the photoexcited hot carriers lose their energy and relax to the bottom of the band over free path, that is, thermalization length (*30*). The relaxation time of the ballistic current $\tau_b \approx 10^{-12} - 10^{-14}$ s $\gg \Omega_B^{-1}$, where $\Omega(= eB/m^*c)$ is the Larmor frequency and B is the classic magnetic field. This permits observation of the Hall effect under illumination for the ballistic linear and circular bulk photovoltaic currents and of the mobility of nonthermalized carriers (*1*, *4*, *30*, *31*).

Shift current is a separate, quantum mechanism whereby accounting for the nondiagonal elements of the density matrix, a consistent kinetic theory was developed (*1*) and later within the framework of density functional theory (*14*, *15*). Shift itself does not have a transport mechanism, it does not involve inertia, and its short (atomic) relaxation time τ_s prevents observation of current kinetics or a photo-Hall effect, because for any classical magnetic field B, $\tau_s \ll \Omega_B^{-1}$. These characteristics explain why shift photovoltaic current has never been observed experimentally despite a number of reports attributing measured photovoltaic currents to shift (*18*–*24*), including transient current measured indirectly from terahertz radiation (*18*, *32*). Also, it was shown that impurity band transitions can contribute to both

shift and ballistic currents and are strongly dependent on the nature of the impurity (*1*).

RESULTS

The ballistic j_b and shift j_s currents are expressed explicitly as $j_b = e\alpha I(\hbar\omega)^{-1} l_0 \xi\phi$ and $j_s = e\alpha I(\hbar\omega)^{-1} R$ (*1*, *4*). Here, ξ is the photoexcitation asymmetry parameter, which is a function of wave vector but is represented here as a scalar. l_0 is the free path of nonthermalized carriers, I is the light intensity, $\hbar\omega$ is the photon energy, α is the absorption coefficient, and ϕ is the quantum yield. The quantity R, called the shift vector, has the meaning of carrier displacement in real space per absorbed photon. Under a very rough approximation $|R| \approx a\xi$, where a is the lattice parameter (for cubic sillenites $a \approx 1$ nm).

The linear BPE current is the sum of the ballistic and shift contributions. It has been shown that the circular BPE current is purely ballistic (*1*, *4*, *33*). To experimentally separate the ballistic and shift currents, we consider here the simultaneous linear and circular currents in a cubic sillenite under magnetic field based on the following relations. The linear bulk photovoltaic current, for example, along [100], is

$$j_l = j_b + j_s \tag{1}$$

The mobility of nonthermalized electrons

$$\mu_{nth} = B^{-1}(j_c^B / j_c) \tag{2}$$

may be obtained from the photo-Hall effect for current collected under circularly polarized light (j_c), where j_c^B is the Hall component under circularly polarized light, and B is the magnetic field applied along [010].

From measurement of the Hall component of linear current j_l^B, we obtain the expressions for ballistic j_b and shift j_s currents

$$j_b = \frac{1}{\mu_{nth} B} j_l^B \tag{3}$$

$$j_s = j_l - \frac{1}{\mu_{nth} B} j_l^B \tag{4}$$

These equations are based on two main theoretical properties (*1*, *4*). First, shift current does not contribute to the Hall signal, and second, the current under circularly polarized light is purely ballistic.

As shown in (*31*, *34*), the magnetic field changes the asymmetry parameter in the Hall direction and could create additional current, which depends linearly on B. Under this condition, the expression for shift current j_s is then

$$j_s(1 + x) = j_l - \frac{1}{\mu_{nth} B} j_l^B \tag{5}$$

where x ($\gtrsim 1$) is a model-dependent parameter characterizing magneto-induced asymmetry [see p. 92 in (*4*)].

We investigated photovoltaic currents in single-crystal, optically active cubic piezoelectric $Bi_{12}GeO_{20}$ (point group T) having one linear component G_{14}^l (in the compact Voigt notation) and one circular component G_{11}^c. A circular and linear BPE in sillenites has been observed previously (*35*). To observe the circular effect, we use an electro-optic modulation technique (*35*, *36*), measuring the linear and circular photovoltaic currents and its Hall component under a magnetic field $B \lesssim 1$ T. The energy gap of $Bi_{12}GeO_{20}$ is ≈3.2 eV (*37*), and we performed the measurements in the extrinsic (impurity) region (450 to 650 nm). It was shown that sillenites have *n*-type photoconductivity (*38*, *39*) arising from Bi^{+3} donors that produce a broad absorption shoulder (≈2.3 to 3.2 eV) (*37*, *40*), and the mobility of thermalized electrons is extremely small ($\mu_{th} \approx 10^{-2} - 10^{-6}$ cm^2 V^{-1} s^{-1}) and depends on the filled trap concentration in the extrinsic region.

Measurements were performed at room temperature (≈300 K) under polarization-modulated monochromatic laser illumination intensities ranging from ≈300 to 2100 mW/cm^2 using commercial single crystals. Photovoltaic currents j_l and j_c were collected through transparent electrodes on the (001) and (00$\bar{1}$) faces, and other electrodes were used to measure their corresponding Hall components j_l^B and j_c^B (Fig. 1, A and B, and Materials and Methods).

The measured absorption spectrum (Fig. 1C) quantifies the extrinsic character in the range studied, where a broad absorption shoulder has been attributed to an antisite defect (Bi_{Ge}) (*37*). The angular dependence of the linear photovoltaic current in [100] $j_l = G_{14}^l \cos(2\beta)$ (β is the angle between the light polarization and [010]) is in agreement with tensorial properties of crystal (Fig. 2A). The obtained spectral dependences of j_l and j_c were collected for a series of wavelengths across the spectral region of $\lambda \approx 450$ to 650 nm (Fig. 2B). Shown in Fig. 2C is the Hall component of the circular photovoltaic current as a function of magnetic field for right (σ^+) and left (σ^-) circularly polarized light for $\lambda = 488.1$ nm. The measurements of j_c and its Hall components indicate that the nonthermalized mobility μ_{nth} approaches 600 cm^2 V^{-1} s^{-1}, exceeding by at least 10^4 the thermalized mobility (*38*, *39*). The high value for nonthermalized carriers has been obtained from photovoltaic Hall measurements for many piezoelectrics and ferroelectrics (*4*, *11*, *41*). The spectral dependence of mobility may be caused by thermalization, related to electron-defect center interaction. The ballistic current j_b is proportional to the product of μ_{nth} and n, the concentration of nonthermalized electrons. We suppose that the minimum in μ_{nth} in the region of the impurity band is due to the stronger interaction of carriers in this spectral region and that n is larger in this spectral range because of the density of impurity centers in this range. These results confirm the extrinsic origin of photovoltaic current by excitation of donor levels and, significantly, that thermalization of nonequilibrium carriers is caused by scattering by ionized impurities. This can explain why the nonthermalized mobility is large outside the impurity band and low within it.

The spectral dependences of j_b and j_s, each normalized to incident power, are presented in Fig. 3A, and corresponding spectral dependences of the tensor (Glass) coefficient G_{14}^l for j_b and j_s are presented in Fig. 3B. Our data and analysis reveal that shift exists in the extrinsic region and that the ballistic and shift currents are of the same order of magnitude, as predicted by theory (*1*, *4*, *14*, *15*), but flow in opposite directions; the latter is a result not anticipated from the theory. The spectral distribution of μ_{nth} has a sharp minimum that is close to the maximum of j_s and j_b (Fig. 3C). It shows, in accordance with (*1*), that in this spectral interval, the impurity band transitions are responsible for ballistic and shift currents, permitting a rough estimate of R. On

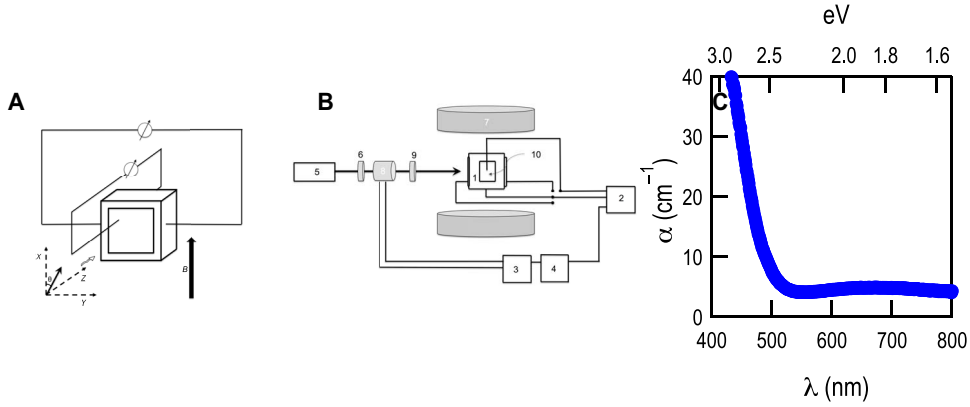

Fig. 1. Experimental scheme for probing bulk photovoltaic current in the extrinsic spectral. (**A**) Schematic illustration of the sample geometry and electrode and field configuration. (**B**) Block diagram illustrating experimental configuration. (1) $Bi_{12}GeO_{20}$ crystal, (2) lock-in amplifier, (3) modulator driving electronics, (4) function generator, (5) Kr/Ar ion laser, (6) polarizer, (7) electromagnet, (8) electro-optic modulator, (9) λ/2 or λ/4 achromatic wave plate, and (10) Hall contacts. (**C**) Measured optical absorption in $Bi_{12}GeO_{20}$.

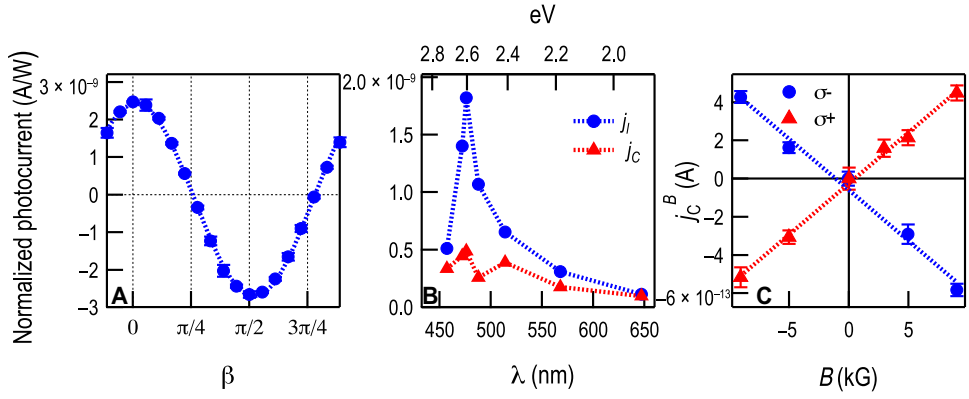

Fig. 2. Bulk photovoltaic currents under linearly and circularly polarized illumination in $Bi_{12}GeO_{20}$, and the corresponding Hall component. (**A**) Measured variation in photocurrent j_l, in $Bi_{12}GeO_{20}$, under linearly polarized λ = 488.1 nm light, as a function of β, the angle between the light polarization and [010]. (**B**) Measured spectral dependences of linear j_l and circular j_c photovoltaic currents, normalized to incident power. (**C**) Hall component of the circular photovoltaic current j_c^B as a function of magnetic field, for right (σ^+) and left (σ^-) circularly polarized λ = 488.1 nm light.

the basis of the data in Fig. 3A, for $\hbar\omega = 2.5$ eV, $R = 0.4 \times 10^{-2}$ nm, and correspondingly, $\xi \approx R/a \approx 0.4 \times 10^{-2}$. This value is in good agreement with the asymmetry parameter obtained for the Coulomb impurity model (*4*). For $\hbar\omega = 2.5$ eV, $\phi l_0 \approx 0.2$ nm, and for $\phi < 1$, l_0 can reach a few nanometers.

DISCUSSION

We note that under small classic magnetic field *B*, no detectable change was observed in j_l or j_c with *B*, and therefore, we conclude that the effect of magneto-induced asymmetry (Eq. 5) is small. The change of j_l^B due to the Faraday effect can be neglected in comparison with the photo-Hall effect. In principle, the mobilities for linear and circular currents are different even in the absence of the magneto-photovoltaic effect. However, following the theory (*1*, *4*, *12*, *33*), this difference is within a factor of two, and accordingly does not influence the value of j_s by more than an order of magnitude. With regard to the validity of Eqs. 2 to 5, it is well established that the photovoltaic current under circularly polarized light in the absence of magnetic field is purely ballistic (injection). While the mechanism for photovoltaic current for circularly polarized light in the presence of a magnetic field may be altered because of the change in the balance between the energy renormalization current and shift current, we have assumed here that in a magnetic field, the photovoltaic current in circularly polarized light remains ballistic and that the Hall mobility under circularly polarized light is ballistic. Last, we note that shift and ballistic currents in the extrinsic regime may be distinguished in other materials. Application of the same method to the sillenite $Bi_{12}SiO_{20}$ also permits their separation, observation of a different sign, but different spectral dependence (Supplementary Materials).

Decades following its discovery and despite a well-developed theoretical framework for shift and ballistic currents, quantifying the extent of their contributions from these coexisting quantum and quasi-classical mechanisms has remained experimentally inaccessible. Analysis of the steady-state linear and circular photovoltaic currents for the separation of shift and ballistic contributions to the photovoltaic current in perovskites and other crystals that belong to 18 optically active point groups, including those of extrinsic origin, is now feasible. We anticipate that facile experimental disambiguation of shift should encourage new exploration of connections of first principles–based

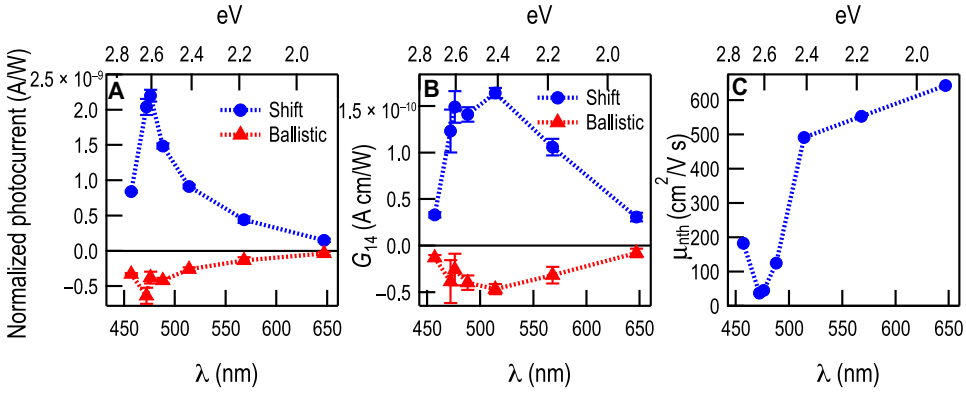

Fig. 3. Separation of shift and ballistic contributions to the bulk photovoltaic current. (**A**) Spectral dependences of shift j_s and ballistic j_b photovoltaic currents, each normalized to incident power. (**B**) Corresponding spectral shift and ballistic Glass coefficients. (**C**) Spectral dependence of the nonthermalized carrier mobility in $Bi_{12}GeO_{20}$.

calculations with experiment. The experimental prescription holds great promise for exploiting these remarkable light-matter interactions and may be helpful in efforts to obtain higher power conversion efficiency in devices based on inversion symmetry breaking of the BPE (*11*, *42*).

MATERIALS AND METHODS

Measurements were performed using commercially sourced (MetaLaser, China) $Bi_{12}GeO_{20}$ single crystals with dimensions of 5 by 5 by 5 mm^3 along the *x*, *y*, and *z* axes, which coincide with < 100 >. Optical absorption of the identical $Bi_{12}GeO_{20}$ crystal was collected using ultraviolet-visible spectrophotometry (Shimadzu 1450). Transparent conducting electrodes (indium tin oxide) were deposited by radio frequency sputtering onto (001) and (00$\bar{1}$) faces to collect j_l and j_c, while other electrodes were used to measure their corresponding Hall components j_l^B and j_c^B. For electro-optic polarization modulation–assisted measurements of linearly and circularly polarized photovoltaic currents, the crystal was illuminated with selected lines from a Kr-Ar ion mixed-gas laser (Coherent Innova I90-6) through an electro-optic modulator permitting generation of positive (σ^+) and negative (σ^-) circular light polarization and, correspondingly, the changed sign of circular current j_c. A linearly polarized beam from the laser is polarization modulated at 41 Hz, resulting in oscillation between two mutually perpendicular states before passing through a wave plate, λ/2 or λ/4 (Thorlabs), providing for measurement of j_l and j_c, respectively. Polarization modulation was achieved using a Pockels cell electro-optic modulator (ConOptics, KD*P 350-50) driven by the amplified output of a function generator using voltage magnitude selected for wavelength-dependent half-wave voltage, where a typical half wave voltage for this model at, for example, 500 nm, is 455 V. The resultant polarization states were studied using an analyzer and phototransistor prior to current measurements in the crystals. Current was recorded using a Stanford Research SR-830 digital lock-in amplifier. This phase-sensitive detector was referenced to the synchronous TTL output from the function generator. Photovoltaic current (Hall current) measurements were recorded with *z*-direction (*x* direction) electrodes under short circuit. Typical settings for the lock-in amplifier include low-pass filtering with 18 dB per decade roll-off, a 3-s integration time constant, and the input impedance from the lock-in amplifier is 1 kilohm (for current measurements). Detailed descriptions of similar modulation current measurement methods can be found elsewhere, for example, in (*28*) and (*29*).

SUPPLEMENTARY MATERIALS

Supplementary material for this article is available at http://advances.sciencemag.org/cgi/content/full/5/1/eaau5588/DC1

Symmetry considerations for separation of ballistic and shift photovoltaic currents

Fig. S1. Experimental separation of shift and ballistic contributions to the bulk photovoltaic current in the extrinsic regime in $Bi_{12}SiO_{20}$.

REFERENCES AND NOTES

1. V. I. Belinicher, E. L. Ivchenko, B. I. Sturman, Kinetic theory of the displacement photovoltaic effect in piezoelectrics. *Zh. Eksp. Teor. Fiz.* **83**, 649–661 (1982).
2. A. A. Grekov, M. A. Malitskaya, V. D. Spitsina, V. M. Fridkin, Photoelectric effects in $A^5B^6C^7$-type ferroelectrics-semiconductors with low-temperature phase transitions. *Kristallografiya* **15**, 500–509 (1970).
3. A. M. Glass, D. von der Linde, T. J. Negran, High-voltage bulk photovoltaic effect and the photorefractive process in $LiNbO_3$. *Appl. Phys. Lett.* **25**, 233 (1974).
4. B. Sturman, V. Fridkin, *The Photovoltaic and Photorefractive Effects in Noncentrosymmetric Materials* (Gordon and Breach, 1992).
5. L. Z. Tan, A. M. Rappe, Enhancement of the bulk photovoltaic effect in topological insulators. *Phys. Rev. Lett.* **116**, 237402 (2016).
6. C.-K. Chan, N. H. Lindner, G. Refael, P. A. Lee, Photocurrents in Weyl semimetals. *Phys. Rev. B* **95**, 041104 (2017).
7. S. Y. Yang, J. Seidel, S. J. Byrnes, P. Shafer, C.-H. Yang, M. D. Rossell, P. Yu, Y.-H. Chu, J. F. Scott, J. W. Ager III, L. W. Martin, R. Ramesh, Above-bandgap voltages from ferroelectric photovoltaic devices. *Nat. Nanotechnol.* **5**, 143–147 (2010).
8. A. Bhatnagar, A. R. Chaudhuri, Y. H. Kim, D. Hesse, M. Alexe, Role of domain walls in the abnormal photovoltaic effect in $BiFeO_3$. *Nat. Commun.* **4**, 2835 (2013).
9. R. Nechache, C. Harnagea, S. Li, L. Cardenas, W. Huang, J. Chakrabartty, F. Rosei, Bandgap tuning of multiferroic oxide solar cells. *Nat. Photonics* **9**, 61–67 (2015).
10. L. Wu, S. Patankar, T. Morimoto, N. L. Nair, E. Thewalt, A. Little, J. G. Analytis, J. E. Moore, J. Orenstein, Giant anisotropic nonlinear optical response in transition metal monopnictide Weyl semimetals. *Nat. Phys.* **13**, 350–355 (2017).
11. J. E. Spanier, V. M. Fridkin, A. R. Rappe, A. R. Akbashev, A. Polemi, Y. Qi, Z. Gu, S. M. Young, C. J. Hawley, D. Imbrenda, G. Xiao, A. L. Bennett-Jackson, C. L. Johnson, Power conversion efficiency exceeding the Shockley–Queisser limit in a ferroelectric insulator. *Nat. Photonics* **10**, 611–616 (2016).
12. V. I. Belinicher, B. I. Sturman, The photogalvanic effect in media lacking a center of symmetry. *Sov. Phys. Uspekhi* **23**, 199 (1980).
13. J. E. Sipe, A. I. Shkrebtii, Second-order optical response in semiconductors. *Phys. Rev. B* **61**, 5337–5352 (2000).
14. S. M. Young, A. M. Rappe, First principles calculation of the shift current photovoltaic effect in ferroelectrics. *Phys. Rev. Lett.* **109**, 116601 (2012).
15. S. M. Young, F. Zheng, A. M. Rappe, First-principles calculation of the bulk photovoltaic effect in bismuth ferrite. *Phys. Rev. Lett.* **109**, 236601 (2012).

16. L. Z. Tan, F. Zheng, S. M. Young, F. Wang, S. Liu, A. M. Rappe, Shift current bulk photovoltaic effect in polar materials—Hybrid and oxide perovskites and beyond. *NPJ Comput. Mater.* **2**, 16026 (2016).
17. A. M. Cook, B. M. Fregoso, F. de Juan, S. Coh, J. E. Moore, Design principles for shift current photovoltaics. *Nat. Commun.* **8**, 14176 (2017).
18. N. Laman, M. Bieler, H. M. van Driel, Ultrafast shift and injection currents observed in wurtzite semiconductors via emitted terahertz radiation. *J. Appl. Phys.* **98**, 103507 (2005).
19. M. Bieler, K. Pierz, U. Siegner, P. Dawson, Shift currents from symmetry reduction and Coulomb effects in (110)-oriented GaAs/$Al_{0.3}Ga_{0.7}As$ quantum wells. *Phys. Rev. B* **76**, 161304 (2007).
20. M. Nakamura, F. Kagawa, T. Tanigaki, H. S. Park, T. Matsuda, D. Shindo, Y. Tokura, M. Kawasaki, Spontaneous polarization and bulk photovoltaic effect driven by polar discontinuity in $LaFeO_3/SrTiO_3$ heterojunctions. *Phys. Rev. Lett.* **116**, 156801 (2016).
21. M. Holtz, C. Hauf, A.-A. Hernández Salvador, R. Costard, M. Woerner, T. Elsaesser, Shift-current-induced strain waves in $LiNbO_3$ mapped by femtosecond x-ray diffraction. *Phys. Rev. B* **94**, 104302 (2016).
22. K. Kushnir, M. Wang, P. D. Fitzgerald, K. J. Koski, L. V. Titova, Ultrafast zero-bias photocurrent in GeS nanosheets: Promise for photovoltaics. *ACS Energy Lett.* **2**, 1429–1434 (2017).
23. M. Nakamura, S. Horiuchi, F. Kagawa, N. Ogawa, T. Kurumaji, Y. Tokura, M. Kawasaki, Shift current photovoltaic effect in ferroelectric charge-transfer complex. *Nat. Commun.* **8**, 281 (2017).
24. N. Ogawa, M. Sotome, Y. Kaneko, M. Ogino, Y. Tokura, Shift current in the ferroelectric semiconductor SbSI. *Phys. Rev. B* **96**, 241203 (2017).
25. J. A. Brehm, S. M. Young, F. Zheng, A. M. Rappe, First-principles calculation of the bulk photovoltaic effect in the polar compounds $LiAsS_2$, $LiAsSe_2$, and $NaAsSe_2$. *J. Chem. Phys.* **141**, 204704 (2014).
26. T. Rangel, B. M. Fregoso, B. S. Mendoza, T. Morimoto, J. E. Moore, J. B. Neaton, Large bulk photovoltaic effect and spontaneous polarization of single-layer monochalcogenides. *Phys. Rev. Lett.* **119**, 067402 (2017).
27. H. Ishizuka, N. Nagaosa, Local photo-excitation of shift current in noncentrosymmetric systems. *New J. Phys.* **19**, 033015 (2017).
28. E. L. Ivchenko, G. E. Pikus, New photogalvanic effect in gyrotropic crystals. *Pis'ma Zh. Eksp. Teor. Fiz.* **27**, 640 (1978).
29. V. M. Asnin, A. A. Bakun, A. M. Danishevskii, E. L. Ivchenko, G. E. Pikus, A. A. Rogachev, Observation of a photo-emf that depends on the sign of the circular polarization of the light. *ZHETF Pis'ma v Redaktsiiu* **28**, 80–84 (1978).
30. Z. Gu, D. Imbrenda, A. L. Bennett-Jackson, M. Falmbigl, A. Podpirka, T. C. Parker, D. Shreiber, M. P. Ivill, V. M. Fridkin, J. E. Spanier, Mesoscopic free path of nonthermalized photogenerated carriers in a ferroelectric insulator. *Phys. Rev. Lett.* **118**, 096601 (2017).
31. E. L. Ivchenko, Y. B. Lyanda-Geller, G. E. Pikus, Magneto-photogalvanic effects in noncentrosymmetric crystals. *Ferroelectrics* **83**, 19–27 (1988).
32. M. Sotome, M. Nakamura, J. Fujioka, M. Ogino, Y. Kaneko, T. Morimoto, Y. Zhang, M. Kawasaki, N. Nagaosa, Y. Tokura, N. Ogawa, *Spectral dynamics of topological shift-current in ferroelectric semiconductor SbSI* (2018); https://arxiv.org/abs/1801.10297.
33. E. L. Ivchenko, *Optical Spectroscopy of Semiconductor Nanostructures* (Alpha Science, 2005).
34. E. L. Ivchenko, Y. B. Lyanda-Geller, G. E. Pikus, R. Y. Rasulov, Magnetically induced photogalvanic effect in semiconductors. *Sov. Phys. Semicond.* **18**, 55–60 (1984).
35. M. P. Petrov, A. I. Grachev, Bulk photogalvanic effects in bismuth silicate ($Bi_{12}SiO_{20}$). *Sov. Phys. Solid State* **22**, 1671–1674 (1980).
36. Y. Kamata, S. Kurimura, Y. Uesu, B. A. Strukov, Method for separating linear and circular photogalvanic effects and its application to ferroelectric lead germanate. *Jpn. J. Appl. Phys.* **33**, 5453 (1994).
37. R. Oberschmid, Absorption centers of $Bi_{12}GeO_{20}$ and $Bi_{12}SiO_{20}$ crystals. *Phys. Status Solidi A* **89**, 263–270 (1985).
38. P. V. Lenzo, Light and electric-field-dependent oscillation of space-charge-limited field current in Bi_{12} GeO_{20}. *J. Appl. Phys.* **43**, 1107 (1972).
39. B. K. Kostyuk, A. Y. Kudzin, G. K. Sokolyanskii, Phototransport in $Bi_{12}SiO_{20}$ and $Bi_{12}GeO_{20}$ single crystals. *Sov. Phys. Solid State* **22**, 1429–1432 (1980).
40. J. Frejlich, *Fundamental Concepts, Holographic Recording and Materials Characterization* (John Wiley & Sons, 2007).
41. S. K. Esayan, E. L. Ivchenko, V. V. Lemanov, A. Yu. Maximov, G. E. Pikus, Anisotropic photoconductivity and magnetic-field-induced photogalvanic effect in $Pb_5Ge_3O_{11}$. *Jpn. J. Appl. Phys.* **24**, 299 (1985).
42. M.-M. Yang, D. J. Kim, M. Alexe, Flexo-photovoltaic effect. *Science* **360**, 904–907 (2018).

Acknowledgments: We thank A. M. Rappe, B. I. Sturman, Yu. B. Lyanda-Geller, and F. J. Ferrone for the fruitful discussions, and we express gratitude to S. Tyagi, C. Consaga, C. J. Hawley, and A. Podpirka for technical assistance. **Funding:** J.E.S. and V.M.F. acknowledge the Office of Naval Research under grant no. N00014-1501102170 and the Air Force Office of Scientific Research under grant no. FA9550-13-1-0124 for support. R.A. was supported by the U.S. Army Research Office under grant no. W911NF-14-1-0500, and A.G.-P. was supported by the NSF under grant no. CBET 1705440. A.M.B. acknowledges additional support from Bucks County Community College. **Author contributions:** V.M.F., A.M.B., R.A., and J.E.S. conceived the idea, designed the experiments, and formulated the interpretation of the data. A.M.B., A.A., and E.S. designed and configured the experimental setup. A.M.B. and R.A. performed the experiments and analysis, with A.G.-P. All authors contributed to the analysis of the data. J.E.S. and V.M.F. wrote the manuscript, and all of the authors edited and commented on it. **Competing interests:** The authors declare that they have no competing interests. **Data and materials availability:** All data needed to evaluate the conclusions in the paper are present in the paper and/or the Supplementary Materials. Additional data related to this paper may be requested from the authors.

Submitted 22 June 2018
Accepted 4 December 2018
Published 11 January 2019
10.1126/sciadv.aau5588

Citation: A. M. Burger, R. Agarwal, A. Aprelev, E. Schruba, A. Gutierrez-Perez, V. M. Fridkin, J. E. Spanier, Direct observation of shift and ballistic photovoltaic currents. *Sci. Adv.* **5**, eaau5588 (2019).

ScienceAdvances

Direct observation of shift and ballistic photovoltaic currents

Aaron M. Burger, Radhe Agarwal, Alexey Aprelev, Edward Schruba, Alejandro Gutierrez-Perez, Vladimir M. Fridkin and Jonathan E. Spanier

Sci Adv **5** (1), eaau5588.
DOI: 10.1126/sciadv.aau5588